

## Original Investigation

# Mutation in *TMEM98* in a Large White Kindred With Autosomal Dominant Nanophthalmos Linked to 17p12-q12

Mona S. Awadalla, MBBS, PhD; Kathryn P. Burdon, PhD; Emmanuelle Souzeau, MSc; John Landers, MBBS, MPH, PhD; Alex W. Hewitt, MBBS, PhD; Shiwani Sharma, PhD; Jamie E. Craig, MBBS, DPhil

**IMPORTANCE** Nanophthalmos is a congenital disorder characterized by small eyes, with the main complications being severe hyperopia and angle-closure glaucoma.

**OBJECTIVE** To perform a clinical and genetic investigation of a large white family with autosomal dominant nanophthalmos.


**DESIGN, SETTING, AND PARTICIPANTS** Detailed clinical evaluation and a genome-wide linkage scan was conducted in the family NNO-SA1. Linkage was evaluated with a 10K single-nucleotide polymorphism array, followed by whole exome sequencing, to identify novel segregating coding variants within the linked region. The candidate gene was screened for mutations in additional independent families by direct sequencing of the coding exons and intron/exon boundaries. The expression pattern of the candidate gene in ocular tissues was analyzed by reverse transcriptase-polymerase chain reaction. Participants were recruited through ophthalmology clinics at Flinders Medical Centre, Adelaide, South Australia, Australia. Nanophthalmos was defined as an axial length less than 20.0 mm and/or refractive error greater than +7.00. Of the 35 available individuals from family NNO-SA1, 16 participants (46%) had a diagnosis of nanophthalmos, with mean refraction of +11.8 D and mean axial length of 17.6 mm. Unaffected unrelated individuals serving as controls were screened for the identified mutation. Additional independent families with clinically diagnosed nanophthalmos were also recruited.

**MAIN OUTCOMES AND MEASURES** Nanophthalmos status.

**RESULTS** Significant linkage was detected on chromosome 17 between single-nucleotide polymorphism markers rs2323659 and rs967293, with a maximum location score of 4.1. Exome sequencing identified a single novel segregating missense variant within the linkage region located in exon 8 of the transmembrane-98 (*TMEM98*) gene c.577G>C (p.Ala193Pro), which was absent in the Exome Variant Server database and among 285 local white individuals serving as controls. The *TMEM98* gene was expressed in all ocular tissues tested including sclera and optic nerve head.

**CONCLUSIONS AND RELEVANCE** A novel gene associated with nanophthalmos, *TMEM98* most likely represents the cause of the disease in this family. To our knowledge, this represents the first gene identified causing autosomal dominant nanophthalmos.

*JAMA Ophthalmol.* 2014;132(8):970-977. doi:10.1001/jamaophthalmol.2014.946  
Published online May 22, 2014.

 Supplemental content at [jamaophthalmology.com](http://jamaophthalmology.com)

**Author Affiliations:** Department of Ophthalmology, Flinders University, Flinders Medical Centre, Adelaide, South Australia, Australia (Awadalla, Burdon, Souzeau, Landers, Sharma, Craig); now also with Menzies Research Institute Tasmania, University of Tasmania, Tasmania, Australia (Burdon, Hewitt); Centre for Eye Research Australia, Royal Victorian Eye and Ear Hospital, University of Melbourne, Melbourne, Victoria, Australia (Hewitt).

**Corresponding Author:** Kathryn P. Burdon, PhD, Menzies Research Institute Tasmania, University of Tasmania, Private Bag 23, Hobart, Tasmania, Australia 7001 ([kathryn.burdon@utas.edu.au](mailto:kathryn.burdon@utas.edu.au)).

**M**icrophthalmia is a developmental disorder consisting of bilaterally small eyes. Posterior microphthalmia and nanophthalmos are 2 subtypes of the disorder.<sup>1</sup> Nanophthalmos is characterized by the axial length of the globe being more than 2 SDs smaller than the normal range (<20 mm in adults),<sup>2</sup> and the cornea and lens are typically of normal size,<sup>3</sup> causing severe hyperopia (farsightedness) of +7.00 diopters (D) or more. The smaller dimensions of the anterior chamber depth cause the irido-corneal angle to be typically narrow. Abnormal thickening of the scleral connective tissue is often also observed.<sup>3,4</sup> The abnormal structure of the anterior chamber observed in nanophthalmos differs from that of posterior microphthalmia, a rare phenotype restricted to the posterior segment of the eye, where the anterior chamber is of normal dimensions.<sup>5-7</sup> A recent study<sup>8</sup> has revealed that eyes with posterior microphthalmia have corneal steepening proportional to the degree of the short axial length, suggesting that both nanophthalmos and posterior microphthalmia are not a distinct phenotype, but they represent a spectrum of high hyperopia. The prevalence of all microphthalmia in Australia is between 0.5 and 1.5 per 10 000 births.<sup>9</sup>

Nanophthalmos can be inherited in either an autosomal dominant or autosomal recessive mode.<sup>2,10</sup> Linkage studies in large families with autosomal dominant nanophthalmos have identified linkage to chromosome 11p in a family from the United States,<sup>11</sup> 2q11-q14 in a Chinese family,<sup>12</sup> and 17p12-q12 also in a Chinese pedigree.<sup>13</sup> To date, additional families showing linkage to these regions have not been reported and the causative genes in families with autosomal dominant nanophthalmos have not been identified.

We describe a large family of British ancestry with autosomal dominant nanophthalmos. We conducted genome-wide linkage analysis in this family, localizing the gene to a region of 16.9 Mb on chromosome 17 (overlapping with the linkage region in the Chinese family<sup>13</sup>) and investigated the genes in the linked region for causative mutations.

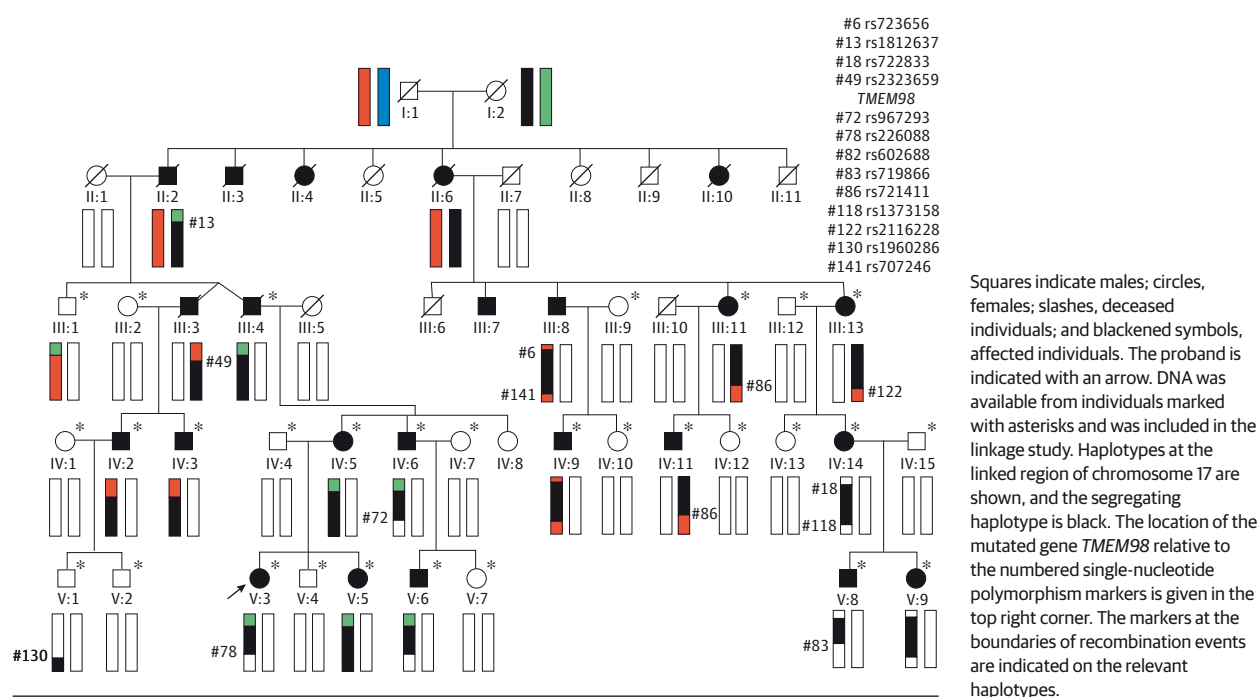
## Methods

### Recruitment of Participants

Family NNO-SA1 (**Figure 1**) was identified following presentation of the proband (V:3) to Flinders Medical Centre, Adelaide, South Australia, Australia, for evaluation and treatment related to angle-closure glaucoma. The primary diagnosis of isolated nanophthalmos was made in that setting by one of the authors (J.E.C.). The family history of this patient was obtained and the extended family was traced for 5 generations. Thirty-five family members were recruited into the study, 16 of whom received a diagnosis of nanophthalmos. An additional 7 family members were reported to have the same phenotype, but were not available for study. The proband and her immediate family reside in Australia; however, much of the extended family is living in the United Kingdom. Written informed consent was obtained from all participants in accordance with the Declaration of Helsinki, and the study was approved by the Southern Adelaide Clinical Human Research Ethics Committee. The participants did not receive financial compensation.

The proband (V:3) received a full ophthalmic examination including refraction, intraocular pressure, central cor-

**Figure 1. Family NNO-SA1 Displaying Autosomal Dominant Nanophthalmos**



neal thickness measurement, slitlamp biomicroscopy, A-scan ultrasonography, and optic disc tomography. Angle-closure glaucoma status was assessed in all participants; however, it was not a part of the criteria used to determine affection status. The rest of the family members were classified as having nanophthalmos if they had an axial length less than 20.00 mm and/or a refractive error at or greater than +7.00. Genomic DNA was extracted from either peripheral whole blood (QiaAmp DNA Blood Maxi Kit; Qiagen) or from saliva (Oragene DNA saliva collection kits; DNA Genotek) according to the manufacturers' protocols.

### Linkage Analysis

All available family members were genotyped (GeneChip Xba 10K single-nucleotide polymorphism [SNP] arrays; Affymetrix Inc) at the Australian Genome Research Facility, Melbourne, Australia. Data were provided in the form of linkage format files, and analyses were conducted in MERLIN, 1.1.2.<sup>14</sup> Because of computational limitations on the number of members of a pedigree, initial genome-wide linkage analysis was conducted using individuals from the proband's branch of the family (descendants of II:1 and II:2), excluding IV:1, V:1, V:2, and V:7, under a fully penetrant dominant model. The disease allele frequency was set to 0.0001 and the allele frequencies for each marker typed were obtained from the CEU collection (white Utah residents with Northern and Western European ancestry from the Centre d'Etude Polymorphism Humain) sample of the International HapMap project (<http://hapmap.ncbi.nlm.nih.gov/>). To confirm the findings, different individuals were excluded and analysis was repeated in the remaining branch of the family (descendants of II:6 and II:7). When the results were compared, only a single region on chromosome 17 showed linkage in both branches. The SNPs surrounding the linked region on chromosome 17 were extracted from the data set, and files were formatted with Mega2<sup>15</sup> for linkage analysis on the entire pedigree in SimWalk2.<sup>16</sup> A fully penetrant dominant model was used to calculate location scores (equivalent to multipoint logarithm of odds scores) and location scores vs chromosome location were plotted. Haplotypes were reconstructed in MERLIN<sup>14</sup> on subsections of the pedigree, with overlapping individuals included in each run to facilitate combining the data into the whole pedigree.

### Exome Sequencing

Sequencing was performed in 5 individuals selected to represent both main branches of the family: 4 affected individuals (IV:2, IV:5, IV:9, and V:9) and 1 unaffected member (IV:4). Enrichment for the exome was performed (TruSeq Exome Enrichment Kit; Illumina Inc) and enriched DNA was sequenced (HiSeq 2000; Illumina Inc) by the Australian Genome Research Facility. Sequence alignment to hg19 was conducted with CASAVA, version 1.8.1 ([https://support.illumina.com/downloads/casava\\_181.ilmn](https://support.illumina.com/downloads/casava_181.ilmn)), and aligner module ELAND, version 2 (Illumina). Realignment and variant calls were made with Illumina Exome Script and variants were annotated by ANNOVAR.<sup>17</sup> All bioinformatics was conducted by the sequencing service provider. The lists of single-nucleotide variants identified in each sample were filtered according to the fol-

lowing criteria: (1) not present in dbSNP131, (2) segregated in the 5 sequenced individuals, and (3) missense, stop, or splice variant.

Segregation in the family was assessed by Sanger sequencing using primer pair exon 8-1 (Supplement [eTable 1]). Polymerase chain reaction (PCR) was performed for each available DNA sample with the following conditions: enzyme activation at 95°C for 15 minutes, 30 cycles of denaturation at 95°C for 30 seconds, annealing at 57°C for 30 seconds, elongation at 72°C for 30 seconds, and final elongation at 72°C for 5 minutes. The PCR products were purified for sequencing using exonuclease I (20 U/μL) and USB Shrimp Alkaline Phosphatase (In Vitro Technologies) (1 U/μL), incubated at 37°C for 60 minutes, and then inactivated at 80°C for 20 minutes.<sup>18</sup> The product was sequenced (BigDye Terminator; Applied Biosystems) on an ABI 3100 DNA sequencer (Applied Biosystems). Chromatograms were compared with each other and the reference sequence (GenBank NM\_001033504.1) (Sequencher, 5.2.3. software; GeneCodes Corp).

The presence of the novel missense variant was tested in 285 individuals serving as controls using a restriction fragment length polymorphism. The cohort was ascertained from retirement villages in Adelaide. The mutation introduces a restriction site for Bsu36I (New England BioLabs Inc). Polymerase chain reaction was performed with the same primers used for sequencing above. A total of 10 μL of PCR product was digested with 2 U of Bsu36I enzyme in the presence of bovine serum albumin. The digested products were visualized under UV light following electrophoresis on 1.4% agarose gel, stained with Gel Red (Biotium). The novel variant was searched against the Exome Variant Server database (<http://evs.gs.washington.edu/EVS/>), a large public data set of unrelated European-American individuals with exome sequence data available.

The functional significance of the mutation in transmembrane-98 (*TMEM98*; GenBank NM\_001033504.1) was analyzed using PolyPhen-2,<sup>19</sup> SIFT using protein ID (ENSP00000261713),<sup>20</sup> and MutationTaster.<sup>21</sup> The conservation of normal *TMEM98* protein was compared between species using data obtained from UniProtKB (<http://www.uniprot.org/uniprot/>) and aligned by ClustalW2.<sup>22</sup>

### Gene Screening in Additional Families With Nanophthalmos

A total of 7 additional independent families with at least 1 affected member participated in the present study. Families were referred to the study from eye clinics in Australia. Extraction and sequencing of the DNA of probands were conducted using the same methods as described above with primers for each coding region of the gene, encompassing splice sites (Supplement [eTable 1]).

### Expression Analysis

Ocular tissues were obtained from postmortem human eyes through the Eye Bank of South Australia according to the guidelines of the Southern Adelaide Clinical Human Research Ethics Committee. Total RNA was extracted from tissues using the RNeasy Micro Kit or Mini Kit (Qiagen). Primers were designed through National Center for Biotech-

Table. Clinical Characteristics of the Affected Family Members

ID	Age, y	BCVA		Refraction, D		Axial Length, mm		IOP, mm Hg		ACG
		RE	LE	RE	LE	RE	LE	RE	LE	
III:4	91	NA	NA	+11.5	NA	NA	NA	NA	NA	NA
III:8	78	6/24	6/30	+15.00	+15.00	18.12	17.92	13	14	No
III:11	86	HM	CF	+9.50	NA	18.02	NA	16	17	Yes
III:13	84	NA	NA	+7.00	+9.50	17.43	17.31	NA	NA	Yes
IV:2	64	6/6	6/9	+11.00	+11.00	17.00	NA	24	24	No
IV:3	49	6/9	6/12	+13.75	+12.87	NA	NA	18	18	NA
IV:5	61	6/48	6/12	+14.00	+15.00	17.10	17.14	33	26	Yes
IV:6	63	NA	NA	+11.87	+12.37	NA	NA	18	19	No
IV:9	52	NA	NA	+9.00	+10.00	NA	NA	NA	NA	NA
IV:11	49	NA	NA	+12.50	+12.00	NA	NA	NA	NA	NA
IV:14	52	6/9	6/36	+14.25	+14.50	NA	NA	NA	NA	Yes
V:3	34	6/60	6/6	+9.75	+10.50	18.46	18.34	42	41	Yes
V:5	26	6/12	6/15	+15.50	+15.00	17.02	16.90	19	18	No
V:6	30	6/6	6/6	+13.25	+13.75	NA	NA	NA	NA	NA
V:8	24	6/12	NLP	+7.50	NA	18.42	NA	40	NA	Yes
V:9	26	NA	NA	+8.25	+8.50	NA	NA	11	11	No

Abbreviations: ACG, angle-closure glaucoma; BCVA, best-corrected visual acuity; CF, counting fingers; D, diopters; HM, hand movements; ID, identification; IOP, highest recorded intraocular pressure; LE, left eye; NA, not available; NLP, no light perception; RE, right eye.

nology Information/Primer-Blast (<http://www.ncbi.nlm.nih.gov/tools/primer-blast/index.cgi?>) for each of the 2 known isoforms: isoform 1 (GenBank NM\_015544) forward primer (5'-3') GCACCTGCCATCCTCTTCCCA and reverse primer (5'-3') GCAGTCGTCCGTGCGTCCAG, and isoform 2 (GenBank NM\_001033504) forward primer (5'-3') GGGAGCCACAGCCTGAGCTTT and reverse primer (5'-3') AGGAGCAGGGCAGTCGTCCG. First-strand complementary DNA was synthesized using the SuperScript III reverse transcriptase (Invitrogen). Polymerase chain reaction was conducted with the following conditions: initial-ization at 95°C for 15 minutes, followed by denaturation at 95°C for 30 seconds, annealing at 62°C for 30 seconds, elongation at 72°C for 30 seconds for 30 cycles using complementary DNA from retina, optic nerve, optic nerve head, ciliary body, and iris, and 32 cycles for sclera, and then a final elongation at 72°C for 5 minutes. The PCR product was visualized on 1.4% agarose gel stained with Gel Red (Biotium). Products were purified for sequencing as described above. The publicly available Illumina Human Body-Map, version 2.0, data were accessed on November 19, 2013, through the Ensembl Genome Browse (<http://www.ensembl.org>) to explore nonocular expression patterns.

## Results

### Recruitment of Participants

Family NNO-SA1 (Figure 1) presented with autosomal dominant nanophthalmos. Sixteen family members were classified as affected (Table). The mean (SD) refraction and axial length of the affected family members were +11.8 (2.5) D and 17.6 (0.6) mm, respectively. Best-corrected visual acuity in these patients ranged from no perception of light to 6/6. Angle-closure glaucoma was detected in 6 of the 16 patients, including the proband (V:3). Individual IV:2 demonstrated slightly

elevated pressure but no sign of glaucoma at the time of recruitment. Other clinical features in affected family members included thick sclera with prominent scleral vessels and an increased frequency of optic disc drusen with some degree of increased vascular tortuosity. There was also a tendency for aqueous misdirection to occur after intraocular surgery, as well as other complications (eg, macular edema and choroidal effusions), often leading to poor outcomes following intraocular surgery for cataract and glaucoma. Representative images of the ocular phenotype are shown in Figure 2.

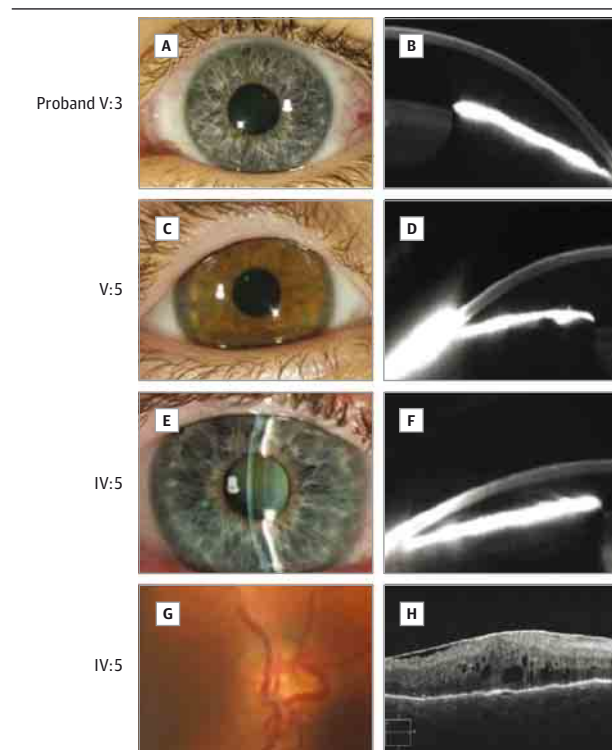
### Linkage Analysis

Linkage analysis in the branch of the pedigree descended from II:1 and II:2 is shown in Figure 3A. Linkage to previously reported nanophthalmos regions on chromosomes 11p<sup>11</sup> and 2q<sup>12</sup> was excluded. Linkage was detected on chromosome 17p12-q12 between SNP markers rs2323659 and rs967293 with a maximum logarithm of odds score of 2.67, overlapping with the region previously identified in the Chinese pedigree.<sup>13</sup> The region was defined by recombination events in individuals III:3 (untyped) and IV:6 (Figure 1). The remaining branch of the family similarly showed linkage to this region on chromosome 17; however, no recombinants were observed that would further refine the linkage region. The linked region is approximately 16.9 megabases (Mb) in physical distance between 15.3 Mb and 32.7 Mb, encompassing the centromere of chromosome 17. Multipoint linkage analysis of this region in the entire family using SimWalk2 gave a location score of 4.1 (Figure 3B).

The 5' boundary marker rs2323659 is located on the p arm of the chromosome. The next informative marker, rs1589464, is separated from the boundary marker by approximately 10 Mb, including the centromere. At the other end of the linked region, the recombination event in individual IV:11 occurred between rs952540 and rs967293. These markers are separated



**Figure 2. Clinical Photos of the Affected Members in the Australian Branch of Family NNO-SA1**



A, C, and E, External eye appearance of patients' nanophthalmos. B, D, and F, Corresponding images obtained with a rotating Scheimpflug camera system (Pentacam; Oculus). Narrow iridocorneal angles and shallow anterior chamber depth were present in all affected eyes. G, The optic disc with the presence of optic disc drusen. H, Optical coherence tomographic image of the macula showing postoperative cystoid macular edema with epiretinal membrane.

by approximately 370 kb, and this region contains minimal annotated genes. Thus, further fine mapping of the linked region is unwarranted.

### Exome Sequencing

All detected variants not present in dbSNP131 are described in the Supplement (eTable 2). Only 3 variants showed segregation in the 5 whole exome-sequenced individuals: rs118038927 at ubiquitin-specific peptidase 22 (*USP22*; GenBank NM\_015276.1), rs139539715 in the noncoding RNA *FOXO3B* (GenBank NR\_026718.1), and a novel variant at *TMEM98*. Of these, rs118038927 is silent and has no predicted effect on protein function and rs139539715 is a common variant (minor allele frequency of 35%). Thus, the novel variant in *TMEM98* is the only variant meeting the criteria for a disease-causing variant. It is a substitution at position c.577G>C (NM\_015544) leading to change of the amino acid alanine to proline at codon 193 (p.Ala193Pro) (Figure 4). This variant was shown by direct sequencing in the remainder of the family to segregate completely with disease. The variant is not present in dbSNP v.137, and was not reported in the Exome Variant Server database (as of March 31, 2014). The mutation introduced a restriction site for Bsu36I resulting in bands of 180 and 420 base pairs (bp) and the undigested wild-type product was 600 bp. The mutation

was not present in 285 unaffected unrelated Australian white controls assessed with this restriction enzyme.

PolyPhen-2, SIFT, and MutationTaster were used to predict the likely pathogenicity of this novel missense variant. MutationTaster predicted it to be a disease-causing variant; SIFT predicted the mutation to be damaging, with a score of 0.05; and PolyPhen-2 predicted this mutation to be possibly damaging, with a score of approximately 60% (sensitivity 81% and specificity 83%) under the HumVar algorithm.<sup>19</sup>

Sequence alignment between multiple species showed a high level of conservation of the *TMEM98* protein in the region of the mutation between mammals, amphibians, and fish. Conservation was less apparent with the one bird species accessed (zebra finch). The wild-type residue was found to be conserved among all vertebrates accessed as shown in the Supplement (eFigure 1).

### Gene Screening in Additional Families With Nanophthalmos

Additional white families with nonsyndromic nanophthalmos were recruited. Of the 22 available family members from 7 families, 13 were affected.

Two families showed autosomal dominant inheritance and, in the remainder, appear to be autosomal recessive. All patients presented with short axial length with a mean of 18.8 (1.2) mm and severe hyperopia with a mean of +8.4 (4) D. No novel variants in *TMEM98* were detected in the probands. All polymorphic variants identified in *TMEM98* in the probands are presented in the Supplement (eTable 3).

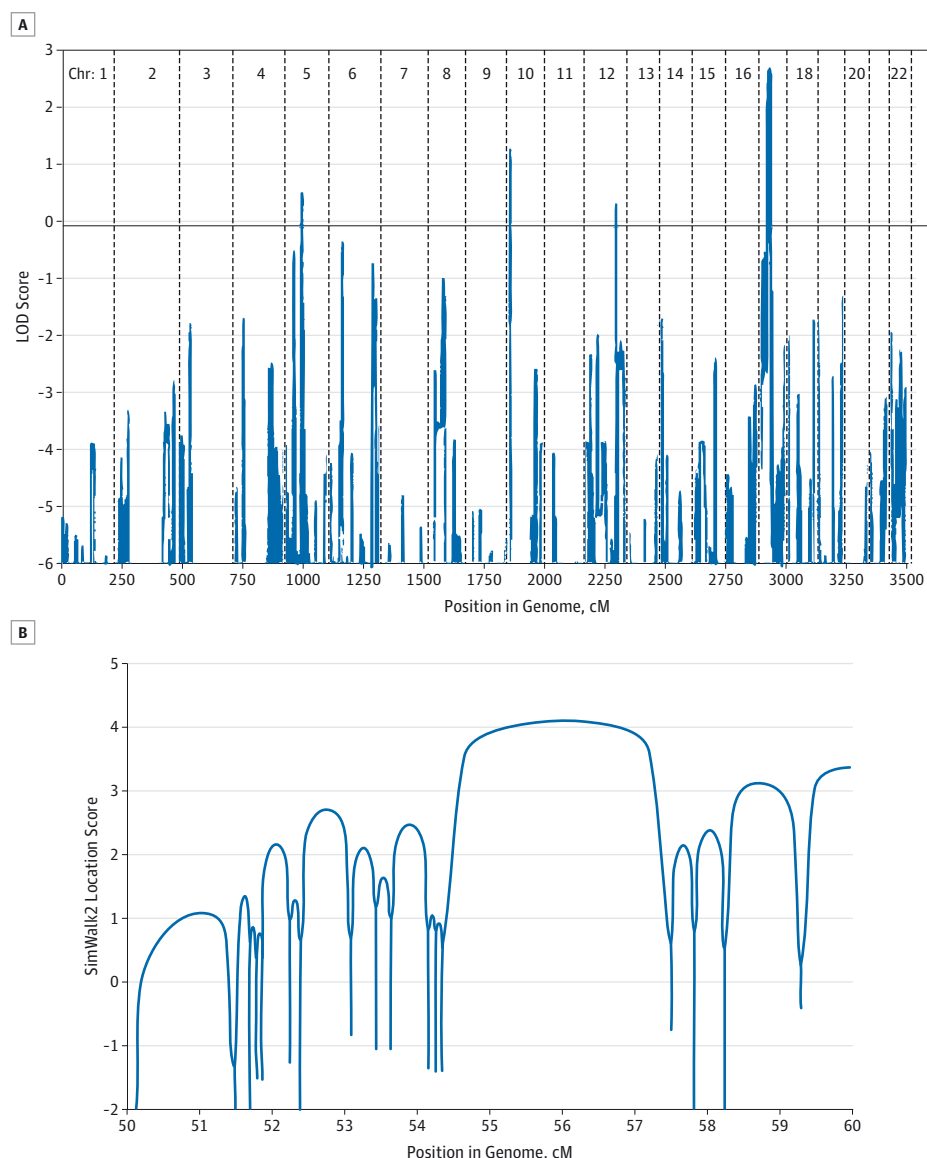
### Expression Analysis

There are 2 reported transcript isoforms of *TMEM98* with different 5' untranslated regions; however, both isoforms encode the same protein. The expression of both transcripts of *TMEM98* in ocular tissues was assessed by reverse transcriptase-polymerase chain reaction (Supplement [eFigure 2]). Both transcripts were expressed in all eye tissues assessed (ie, corneal endothelium, iris, ciliary body, sclera, optic nerve, optic nerve head, and retina) and resulted in products of the expected size (576 bp for isoform 1 and 562 bp for isoform 2). Direct sequencing revealed complete alignment with the reference sequence, confirming the specificity of the products. Ocular expression was further confirmed using The Ocular Tissue Database (<https://genome.uiowa.edu/otdb/>), which showed the expression of *TMEM98* to be high in sclera, choroid RPE, iris, and ciliary body, which are believed to be involved in the pathogenesis of nanophthalmos.<sup>23</sup> According to the Illumina Human BodyMap data, *TMEM98* is expressed in all 16 tissues tested, including adrenal, adipose, brain, breast, colon, heart, kidney, liver, lung, lymph, ovary, prostate, skeletal muscle, testes, thyroid, and white blood cells.

### Discussion

In the present study, we evaluated a large pedigree of white background with autosomal dominant nanophthalmos, identifying a coding mutation in the *TMEM98* gene on chromosome 17 that likely accounts for the phenotype. The single novel

Figure 3. Linkage Analysis of Family NNO-SA1

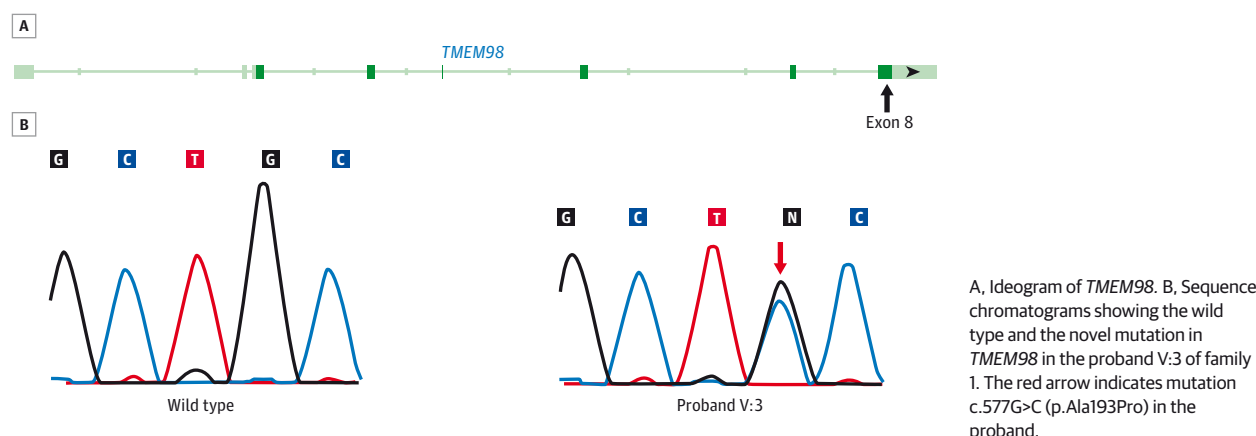


A, Linkage plot showing logarithm of odds (LOD) scores across the whole genome for the descendants of II:1 and II:2. A suggestive peak was identified on chromosome (Chr) 17. B, Linkage plot showing multipoint LOD scores (SimWalk2 location scores) for the linked region of chromosome 17 (between 50 and 60 cM) in the entire family. A maximum score of 4.1 was noted at marker rs952581.

segregating missense mutation, p.Ala193Pro in *TMEM98*, is predicted to be damaging. Given the lack of other segregating putatively functional variants, p.Ala193Pro is likely to be the causative mutation in family NNO-SA1. In addition, the mutation was not detected in 285 individuals serving as controls, and it is not present in large public databases, strengthening the hypothesis that *TMEM98* is the most likely cause of nanophthalmos in this family. However, the absence of pathogenic variants in additional families with nanophthalmos suggests that other genetic loci for this disorder are yet to be identified and replication of this finding in an independent family is yet to occur.

The *TMEM98* gene is expressed in all eye tissues that were assessed in the present study as well as in all the human tissues tested in the Illumina BodyMap project. This ubiquitous expression suggests a fundamental role in cellular processes; however, systemic effects of the mutation in family NNO-SA1

were not noted. Tissue-specific effects may develop through interaction with other ocular-specific transcripts during ocular development or through tissue-specific splicing and regulatory mechanisms. Both isoforms analyzed were expressed in the sclera. This is significant because sclera is abnormally thick in family NNO-SA1 and in patients with nanophthalmos in general. The gene was also expressed in tissues of the iridocorneal angle including the iris and ciliary body. This expression indicates that *TMEM98* might be involved in causing angle-closure glaucoma in patients with nanophthalmos. Very little is known about the function of *TMEM98*. The encoded protein is 226 amino acids long, is leucine rich (13.3%), and is highly acidic, with a theoretical pI of 4.81<sup>24</sup>; it has been detected in most healthy tissues (localized to the nucleus and cytoplasm) as well as in cancers (<http://www.proteinatlas.org/ENSG0000006042/tissue>).

Figure 4. Mutation Located in Exon 8 of *TMEM98*

A similar linkage region, ranging from 14.1 Mb to 33.0 Mb on chromosome 17, has been reported<sup>13</sup> in autosomal dominant congenital simple microphthalmia in a Chinese family. The region reported in our study is entirely encompassed within the previously reported region. The overall phenotype appears similar to that described in the linked Chinese family,<sup>25</sup> although the white family has slightly worse refraction (mean, +11.8 D vs +8.0 D) and correspondingly slightly shorter axial length (mean, 17.6 mm vs 19.2 mm). Rates of glaucoma are similar between the 2 families. The distinction between nanophthalmia and microphthalmia is likely to be arbitrary; however, molecular genetic diagnosis may help better define such overlapping conditions. It is possible that the caus-

ative gene is different between the 2 families, but it is highly likely that both conditions are caused by a mutation in the same gene within the smaller region defined by the white family reported in the present study.

## Conclusions

To our knowledge, this is the first study to report mutations in *TMEM98* and to link this gene to a disease. Additional in-depth investigations are required to explore the involvement of *TMEM98* in normal eye development and determine its role in the pathogenesis of nanophthalmos.

## ARTICLE INFORMATION

**Submitted for Publication:** August 13, 2013; final revision received January 23, 2014; accepted February 2, 2014.

**Published Online:** May 22, 2014.  
doi:10.1001/jamaophthalmol.2014.946.

**Author Contributions:** Drs Awadalla and Burdon contributed equally to the study. Dr Burdon had full access to all the data in the study and takes responsibility for the integrity of the data and the accuracy of the data analysis.

**Study concept and design:** Awadalla, Burdon, Landers, Hewitt, Craig.

**Acquisition, analysis, or interpretation of data:** All authors.

**Drafting of the manuscript:** Awadalla, Burdon, Sharma, Craig.

**Critical revision of the manuscript for important intellectual content:** All authors.

**Statistical analysis:** Awadalla, Burdon.

**Obtained funding:** Craig.

**Administrative, technical, or material support:** Souzeau, Craig.

**Study supervision:** Burdon, Hewitt, Sharma, Craig.

**Conflict of Interest Disclosures:** None reported.

**Funding/Support:** This work was funded by a grant from Flinders University and the Ophthalmic Research Institute of Australia and by grant GNT1023911 from the National Health and Medical Research Council (NHMRC) Centre for Research Excellence (Dr Burdon). Dr Burdon receives funding

from an NHMRC of Australia Career Development Award, and Dr Craig is an NHMRC practitioner fellow.

**Role of the Sponsor:** The sponsors had no role in the design and conduct of the study; collection, management, analysis, and interpretation of the data; preparation, review, or approval of the manuscript; and decision to submit the manuscript for publication.

**Additional Contributions:** We thank the families who contributed samples for this project. We are grateful to the ophthalmologists who assisted with patient and family recruitment: Robert Casson, MBBS, DPhil, FRANZCO (FRANZCO, South Australian Institute of Ophthalmology, Adelaide), Mark Walland, MBBS, FRANZCO (University of Melbourne, Melbourne), Guy D'Mellow, MBBS, FRANZCO (Terrace Eye Centre, Brisbane, Queensland), Richard Mills, MBBS, PhD, FRANZCO (Flinders University, Adelaide), Stewart Lake, MBBS, FRANZCO (Flinders University), Michael Coote, MBBS, FRANZCO (Melbourne Eye Specialists, Melbourne), Anna Galanopoulos, MBBS, FRANZCO (South Australian Institute of Ophthalmology), and Erica Mancel, MD, FRANZCO, CHT (Gaston Bourret Medical Centre, Noumea, New Caledonia). The contributors did not receive financial compensation.

**Correction:** This article was corrected on May 29, 2014, to fix the byline.

## REFERENCES

1. Said MB, Chouchène E, Salem SB, et al. Posterior microphthalmia and nanophthalmia in Tunisia caused by a founder c.1059\_1066insC mutation of the *PRSS56* gene. *Gene*. 2013;528(2):288-294.
2. Vingolo EM, Steindl K, Forte R, et al. Autosomal dominant simple microphthalmos. *J Med Genet*. 1994;31(9):721-725.
3. Sundin OH, Dharmaraj S, Bhutto IA, et al. Developmental basis of nanophthalmos: MFRP is required for both prenatal ocular growth and postnatal emmetropization. *Ophthalmic Genet*. 2008;29(1):1-9.
4. Sundin OH, Leppert GS, Silva ED, et al. Extreme hyperopia is the result of null mutations in *MFRP*, which encodes a frizzled-related protein. *Proc Natl Acad Sci U S A*. 2005;102(27):9553-9558.
5. Khan AO. Recognizing posterior microphthalmos. *Ophthalmology*. 2006;113(4):718.
6. Khairallah M, Messaoud R, Zaouali S, Ben Yahia S, Ladjimi A, Jenzri S. Posterior segment changes associated with posterior microphthalmos. *Ophthalmology*. 2002;109(3):569-574.
7. Spitznas M, Gerke E, Bateman JB. Hereditary posterior microphthalmos with papillomacular fold and high hyperopia. *Arch Ophthalmol*. 1983;101(3):413-417.
8. Nowlaty SR, Khan AO, Aldahmesh MA, Tabbara KF, Al-Amri A, Alkuraya FS. Biometric and molecular characterization of clinically diagnosed posterior

- microphthalmos. *Am J Ophthalmol*. 2013;155(2):361-372.e7. doi:10.1016/j.ajo.2012.08.016.
9. Castilla EE, Botto LD. *Annual Report 2010 With Data for 2008*. Rome, Italy: International Clearing House for Birth Defects Surveillance and Research; 2010.
  10. Martorina M. Familial nanophthalmos [in French]. *J Fr Ophtalmol*. 1988;11(4):357-361.
  11. Othman MI, Sullivan SA, Skuta GL, et al. Autosomal dominant nanophthalmos (NNO1) with high hyperopia and angle-closure glaucoma maps to chromosome 11. *Am J Hum Genet*. 1998;63(5):1411-1418.
  12. Li H, Wang JX, Wang CY, et al. Localization of a novel gene for congenital nonsyndromic simple microphthalmia to chromosome 2q11-14. *Hum Genet*. 2008;122(6):589-593.
  13. Hu Z, Yu C, Li J, et al. A novel locus for congenital simple microphthalmia family mapping to 17p12-q12. *Invest Ophthalmol Vis Sci*. 2011;52(6):3425-3429.
  14. Abecasis GR, Cherny SS, Cookson WO, Cardon LR. MERLIN—rapid analysis of dense genetic maps using sparse gene flow trees. *Nat Genet*. 2002;30(1):97-101.
  15. Mukhopadhyay N, Almasy L, Schroeder M, Mulvihill WP, Weeks DE. Mega2: data-handling for facilitating genetic linkage and association analyses. *Bioinformatics*. 2005;21(10):2556-2557.
  16. Sobel E, Lange K. Descent graphs in pedigree analysis: applications to haplotyping, location scores, and marker-sharing statistics. *Am J Hum Genet*. 1996;58(6):1323-1337.
  17. Wang K, Li M, Hakonarson H. ANNOVAR: functional annotation of genetic variants from high-throughput sequencing data. *Nucleic Acids Res*. 2010;38(16):e164. doi:10.1093/nar/gkq603.
  18. Bell J. A simple way to treat PCR products prior to sequencing using ExoSAP-IT. *Biotechniques*. 2008;44(6):834.
  19. Adzhubei IA, Schmidt S, Peshkin L, et al. A method and server for predicting damaging missense mutations. *Nat Methods*. 2010;7(4):248-249.
  20. Kumar P, Henikoff S, Ng PC. Predicting the effects of coding non-synonymous variants on protein function using the SIFT algorithm. *Nat Protoc*. 2009;4(7):1073-1081.
  21. Schwarz JM, Rödelsperger C, Schuelke M, Seelow D. MutationTaster evaluates disease-causing potential of sequence alterations. *Nat Methods*. 2010;7(8):575-576.
  22. Larkin MA, Blackshields G, Brown NP, et al. Clustal W and Clustal X version 2.0. *Bioinformatics*. 2007;23(21):2947-2948.
  23. Wagner AH, Anand VN, Wang WH, et al. Exon-level expression profiling of ocular tissues. *Exp Eye Res*. 2013;111:105-111.
  24. Wilkins MR, Gasteiger E, Bairoch A, et al. Protein identification and analysis tools in the ExPASy server. *Methods Mol Biol*. 1999;112:531-552.
  25. Yu C, Hu Z, Li J, Liu T, Xia K, Xie L. Clinical and genetic features of a dominantly-inherited microphthalmia pedigree from China. *Mol Vis*. 2009;15:949-954.